SACLANTCEN REPORT
serial no: SR- 320

SACLANT UNDERSEA RESEARCH CENTRE REPORT

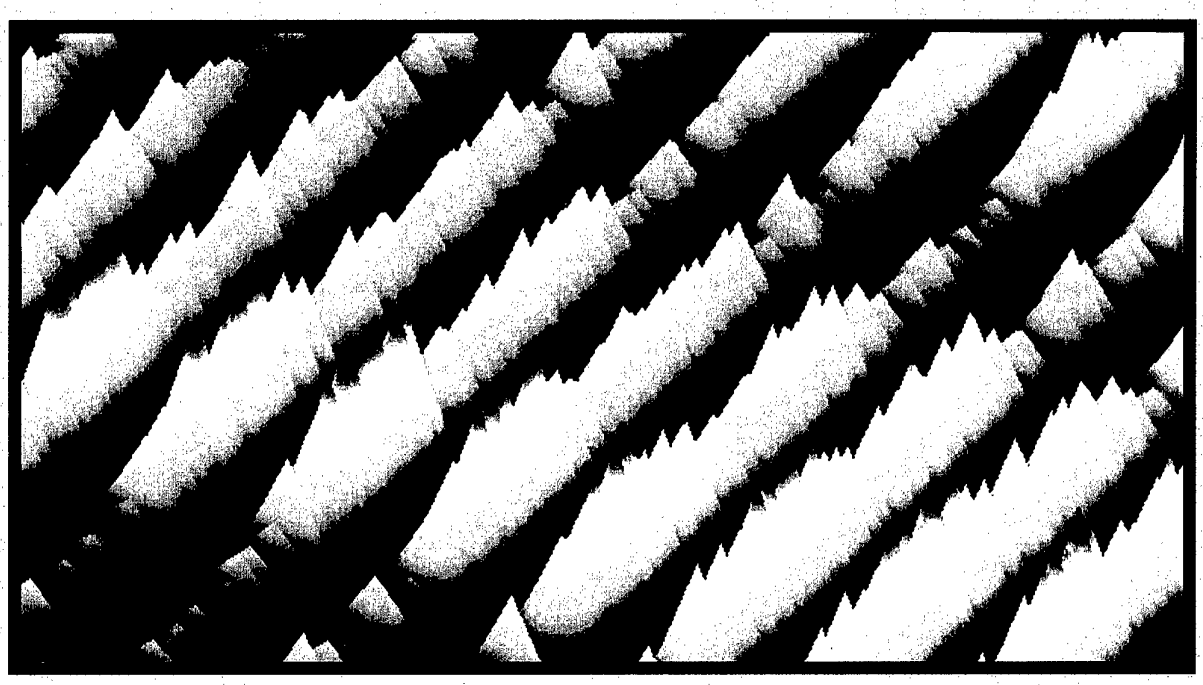

DISTRIBUTION STATEMENT A
Approved for Public Release
Distribution Unlimited

NORTH ATLANTIC TREATY ORGANIZATION ORGANISATION DU TRAITE DE L'ATLANTIQUE NORD

SWAC 4: Broadband data analysis using sub-band processing

G. Haralabus, E. Capriulo,
and W. M. X Zimmer

The content of this document pertains to work performed under Project 04-A of the SACLANTCEN Programme of Work. The document has been approved for release by The Director, SACLANTCEN.

Jan L. Spoelstra
Director

intentionally blank page

SWAC 4: Broadband data analysis using sub-band processing

G. Haralabus, E. Capriulo, and W. M. X Zimmer

Executive Summary:

Broadband signal processing is gaining attention in the underwater research community as it demonstrates system performance enhancement in cluttered, littoral waters. The analysis of wide band signals has significant potential in target detection, multistatic sensing, and modelling. Early experiments demonstrated that bandwidth increase improves target detection in reverberation limited conditions, an issue of extreme importance to Fleet applications. In a multi-sensor, multi-platform configuration, frequency incompatibility problems can be avoided by utilizing broadband instruments. A wide spectrum may also be used to counter counter-measures by changing operational frequencies to combat jammers. Finally, sound propagation and target modelling programmes could utilize broadband signals to simulate a wider variety of scenarios and improve verisimilitude to real life conditions. SACLANT centre is presently acquiring its own experimental broadband sonar and will exercise its first sea trial dedicated to broadband processing in November 1999.

Here, broadband data sets from the SWAC 4 sea trial were used to investigate the frequency dependence of detection performance during this experiment. A sub-band matched filter scheme is deviced. The 1200-Hz transmitted signal is divided ten equal sub-bands, each of which is processed individually. Ultimately this method may lead to optimum operational frequency selection. The data set demonstrates comparable detection performance across the spectrum. The signal-to-noise ratio as a function of frequency is also examined. Frequency shift and sub-band synchronization problems created by long duration active transmissions are addressed. Finally, a method is developed for range rate estimation (relative velocity between source and receiver) based on intra-ping differential time delay of sub-band detection outputs.

intentionally blank page

SWAC 4: Broadband data analysis using sub-band processing

G. Haralabus, E. Capriulo, and W. M. X Zimmer

Abstract:

The frequency dependence of broadband active detection/localization is examined. The analysis is based on 1200 Hz (2300-3500 Hz) LFM signals acquired during the SWAC 4 sea trial. A sub-band matched filter scheme is devised according to which a replica of the transmitted pulse is segmented into ten 120 Hz sub-bands and processed independently through a matched filter detector. Comparison of target detection and ranging results indicate comparable performance for all sub-bands. However, ping-to-ping variability of the ten correlator outputs suggest that the detection performance may be improved by employing incoherent processing schemes. Signal-to-noise ratio is proved to be controlled mainly by noise (reverberation is the predominant noise source) rather than signal variations. The signal intensity remains proportional to the distance between source and receiver due to favorable propagation conditions. Doppler effects and sub-band detection synchronization problems which may lead to performance degradation in large time-bandwidth signal processing are addressed. A method to estimate range rate (relative velocity between source and receiver) based on single ping differential time delay between sub-band MF outputs is developed. This intra-ping technique is an alternative to the standard inter-ping method which requires multiping detection history.

Keywords:

Broadband, sub-band processing, detection variability, intra-ping differential time delay, range rate

Contents

1

Introduction

The increased utilization of broadband signals in anti-submarine warfare is related to sonar performance enhancement in littoral waters, optimum operational frequency selection, multi-purpose experimental settings and new research developments. Preliminary wide band experiments indicate potential performance improvement in reverberation limited environments. Large bandwidth implies small resolution cells and concomitant reverberation suppression, which leads to target detection enhancement [1], [2], [3]. Additionally, multistatic experiments require transmitting and receiving devices on different platforms. It is highly improbable that all assets operate at the same frequencies. The utilization of broadband signals offers the opportunity to select a common operating spectrum segment which guarantees frequency compatibility.

Detection performance may be enhanced by optimum operating frequency selection, advanced incoherent processing, and waveform [4] and filter optimization techniques [5]. The waveform optimization method is based on adaptive pulse length correction which works by allocating energy to frequency bands according to *in situ* measured reverberation and ambient noise spectra. This requires a continuing adaptation of the replica pulse during the experiment based on environmental input. The filter optimization method works by pre-whitening the received signal and assumes knowledge of the noise spectrum. Both these methods are susceptible to environmental mismatch.

Modelling of a wide band active sonar scenario is a very complex task. There is no simulation toolkit which offers an accurate and robust, end-to-end solution to target detection based on broadband medium modelling. The main reason for this is that research tends to focus on different modules of the simulation chain independently of overall compatibility. For the time being, broadband processing payoffs will probably be demonstrated in experiments at sea. SACLANT centre is presently acquiring its own experimental broadband sonar and will exercise its first sea trial dedicated to broadband processing in November 1999.

The purpose of this project is to exploit broadband active signals to measure detection performance, optimum operational frequency, and the development of methods suitable for optimizing the (incoherent) processing gain of wide band signals.

As an early approach into broadband processing analysis, data from the SWAC 4 sea trial are analyzed. Broadband signals of 1200 Hz bandwidth (centered around 3 KHz) were used. The goal here is to assess the frequency dependence of matched filtering (MF) when applied to broadband signals. A sub-band matched filter (MF) processing scheme is deviced. A replica of the 1200 Hz transmitted signal is divided into ten sub-bands and the MF algorithm is applied to each sub-band. Comparison between the various outputs reveals the frequency dependence of the detection results. Aspects of the sub-band detection examined here are: sub-band target detection/localization, signal-to-noise ratio (SNR) comparison, Doppler and sub-band synchronization, and intra-ping range rate estimation.

2

Experimental configuration and data acquisition

The data processed were acquired during run 18 of the SWAC 4 sea trial which took place in the Ionian sea in 1996. Figure 1 shows the bathymetry of the area. The coordinates of the course of the R.V. Alliance and the target are shown in Fig. 2. It is a typical closing-opening range type of run. The minimum and maximum ranges between source and target are 7.9 km and 31.4 km respectively. The target depth is approximately 70 m, the source depth is 68 m and the towed array depth is 64 m. A variation of the order two meters from these nominal values is expected due to undersea currents, velocity changes of the towing ship, and instrument inaccuracies.

The run continued for approximately 2:30 hours; commencing 05:51 ending 08:06 Zulu time. A total of 180 pings were transmitted. At the transmission of the 15th ping (closing part), the coordinates of the Alliance were 37:35.914 N, 21:14.41 E, the speed was 5.2 kn, the heading 112.5 degrees, and the array heading 111.2 degrees. During the opening part, when the 150th ping was transmitted Alliance was at 37:31.65 N, 21:28.576 E, speed 5.2 kn, heading 113.3 degrees, and array heading 111.6 degrees.

The transmitted signal is a 12 s, uniform LFM with frequencies 2300 Hz to 3500 Hz. The receiving device is a 64-element, mid frequency, horizontal array. 21 beams are formed. The sampling frequency is 4000 Hz. The length of the acquisition window is 55 s (including the 12 s transmission) plus a 5 s waiting period which results in a one ping per minute repetition rate.

The general propagation conditions in the area are shown in Fig. 3 and Fig. 4. The three sound velocity profiles correspond to a) the beginning of the run (37:36.589 N, 21:12.265 E), b) approximately at the middle of the run (37:33.632 N, 21:21.984 E), and c) towards the end of the run (37:30.988 N, 21:30.670 E). They are typical, downward refracting, Mediterranean summer profiles [6]. Compared to the two profiles of the shallow water zone, the deep water profile Fig. 3 a) demonstrates shallow surface layer and main thermocline layer with increased negative sound speed slope.The propagation loss plots created using the C-SNAP simulation package [7] are shown in Fig. 4 and 5. The source is placed at 68 m depth. Figure 4 shows a five-frequency propagation loss average of the lowest sub-band 2300-2420 Hz for each one of the three sound velocity profiles. Figure 5 shows the corresponding five-frequency propagation loss average for the highest sub-band 3380-3500 Hz. For

the first profile, the deep water in conjunction with the source placement at the negative gradient part of the sound velocity profile results in wide acoustic energy distribution in the first 20 km. For the other two cases, the source is situated at the isothermal part of the sound velocity thus creating a distinct, long-range channel axis.

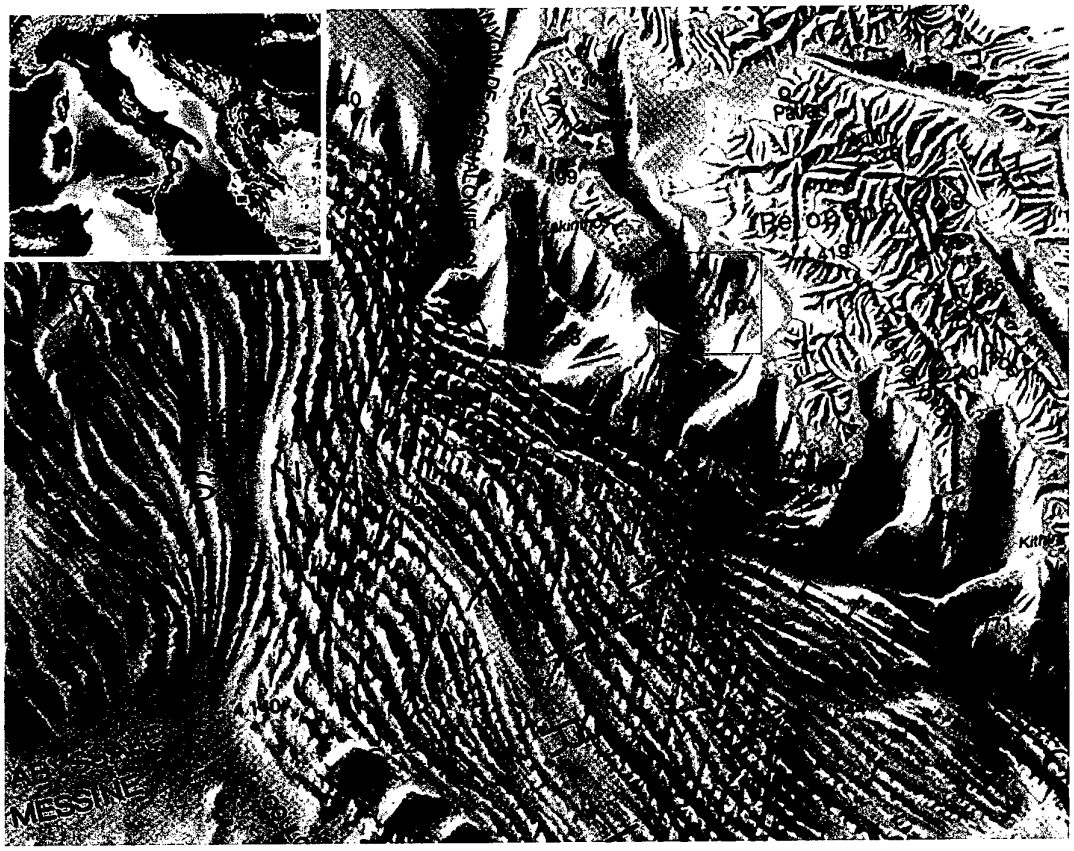

Figure 1: Experimental site for the SWAC 4 trial.

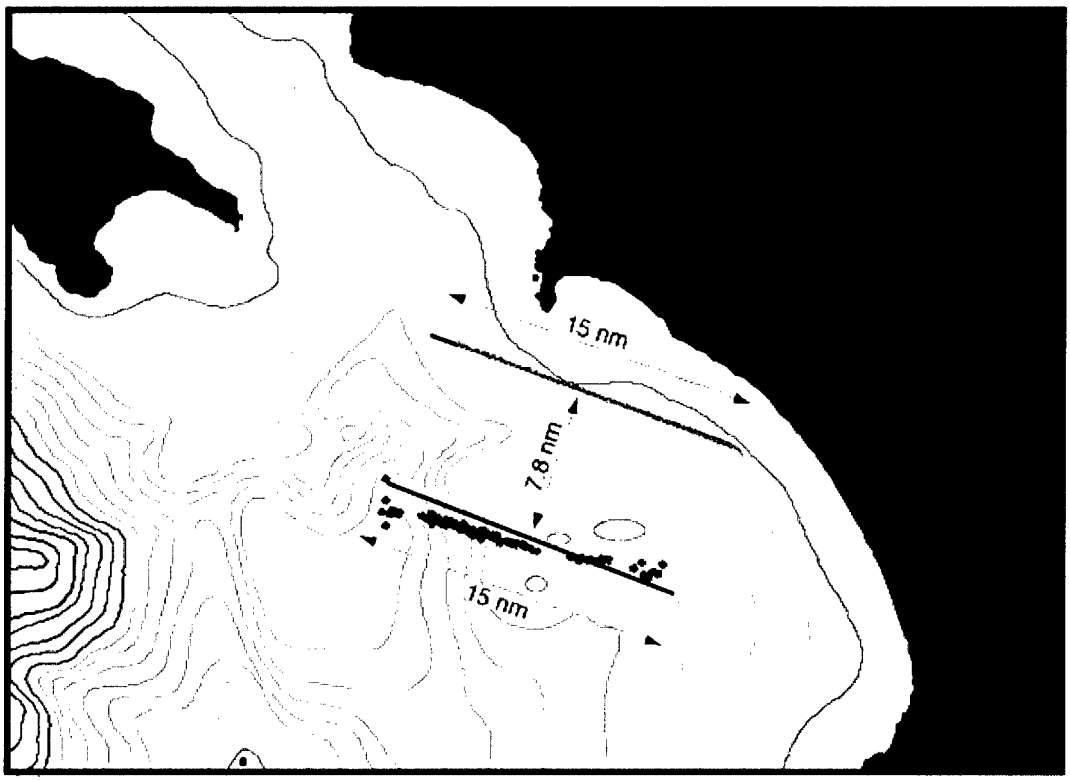

Figure 2: Geometry of run 18 of the SWAC4 sea trial.

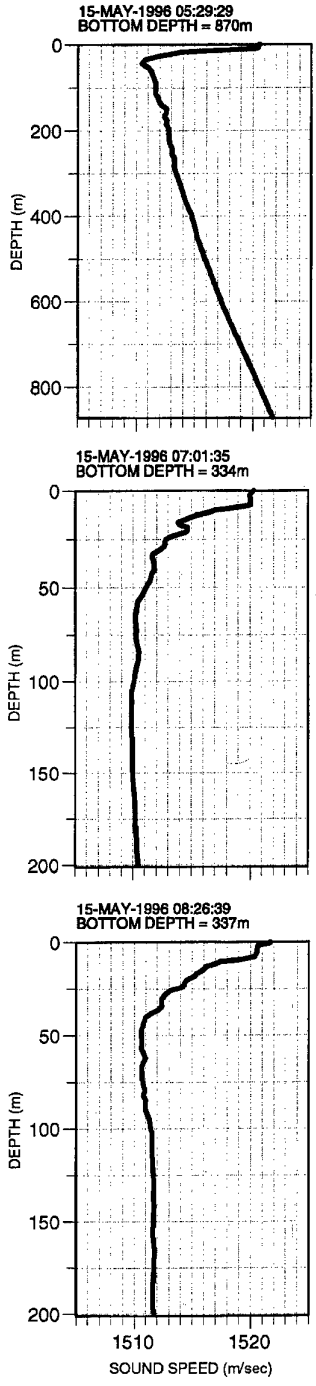

Figure 3: Sound velocity profiles measured during run 18 of the SWAC 4 sea trial.

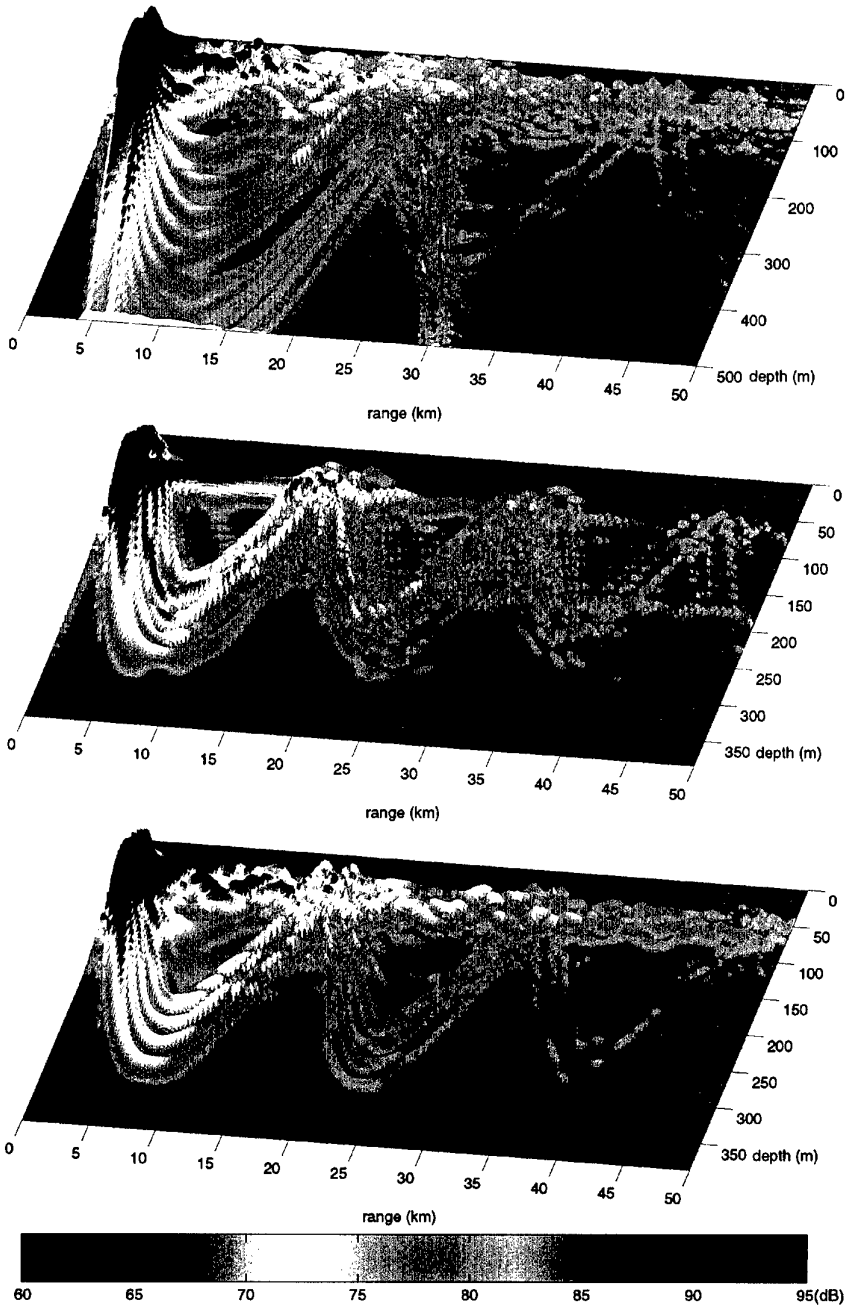

Figure 4: Five-frequency average propagation loss plots for the lower end of the spectrum. The central frequency used in the simulation is 2360 Hz.

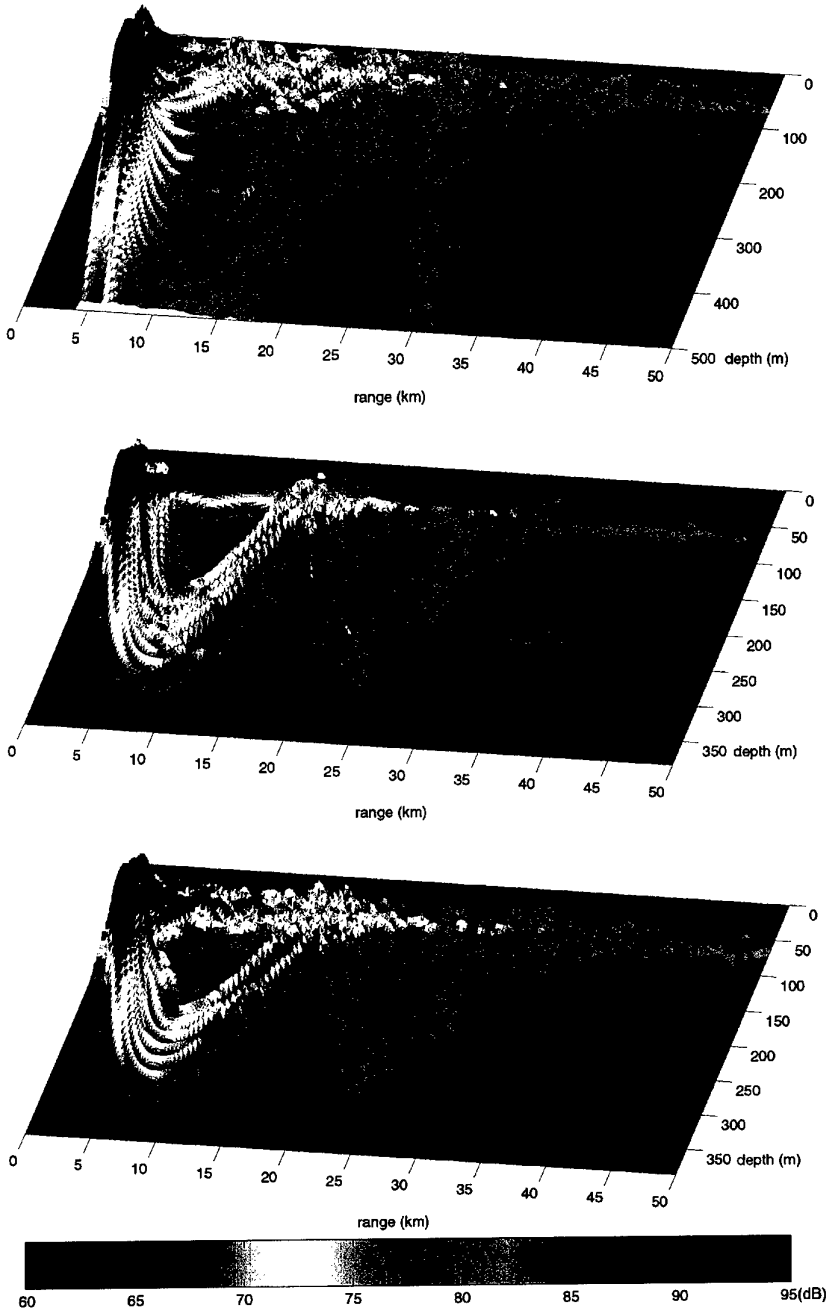

Figure 5: Five-frequency average propagation loss plots for the higher end of the spectrum. The central frequency used in the simulation is 3440 Hz.

3

Target detection/localization based on sub-band processing

The transmitted LFM spectrum ranges from 2300 to 3200 Hz. This 1200 Hz band is divided into ten sub-bands and ten LFM replicas of 120 Hz bandwidth are created. The replicas are correlated with the full band of the received signal using the MF algorithm. For each ping the beam with the highest SNR is chosen. The results are arranged in a ten-segment detection output series (Fig. 6) of unnormalized data. The main goal is to explore the similarities and the diversities of the sub-band detection outputs based on a qualitative and quantitative comparison, with emphasis on frequency dependent trends which may indicate ways to exploit detection results in a coherent or incoherent manner.

The partition of the LFM signal into ten segments is meaningful from an energy point of view because the 12 s duration of the pulse allocates sufficient (for detection purposes) energy to each sub-band. Figure 7 displays the five sub-band MF output of the low frequencies, and Fig. 8 shows the five sub-band MF outputs of the high frequencies (notice that Fig. 7 and Fig. 8 are emphasized segments of Fig. 6). 51 pings (from 40 to 90) are displayed for each sub-band corresponding to the part of the run before, during, and after the closest point of approach (CPA). The x-axis represents the range between source and target and the y-axis shows the magnitude of the unnormalized data. In general, the MF outputs are similar in the sense that there is not a particular band in which the detection performance is distinctly different from the rest. This implies that the frequency dependence is not significant. However, a ping-to-ping comparison reveals many discrepancies. For the same range, the local sub-band maxima usually correspond to different pings. It is interesting to note that the absolute maximum does not correspond to the CPA, although at this point the target aspect is broadside and the distance between source and target is minimized.

Figure 9 is another way of looking at target detection results for all sub-bands. It is a pseudo 3-D plot with the plane axis showing range in km versus ping number. The "hidden" third dimension is the size of the dot which is proportional to the signal-to-noise (SNR) ratio and varies from 10 dB (detection threshold) to 48 dB. The lowest plot corresponds to the lowest frequency band. The other plots are arranged with increasing frequency order. An artificial displacement of 1 km between adjacent bands is set to avoid overlapping.

The pattern of localization is similar to the previous results. In Fig. 9 it is also observed that the closing and the opening part of the run (pings 20 to 80 (=CPA) and pings 81 to 150 respectively) do not have symmetric values around the CPA. That SNR values peak at the closing part of the run before reaching the CPA, is attributed to ambient noise and mainly reverberation fluctuations, as discussed in the following section.

Figure 10 is a 3-D plot of the SNR as a function of frequency. It is found that reverberation is the principle source of noise during the run. The ping average SNR is also indicated for each sub-band. The mean of the average SNR of the five high frequency sub-bands is 31.6 dB and that of the five low frequency bands is 30.6 dB. This difference is attributed to the array gain variation with frequency. As the frequency is decreased below the critical frequency for which $\lambda = 2d$, the array gain decreases approximately 3 dB per octave.

Target detection/localization based on coherent, full bandwidth MF processing is not considered due to severe motion effect. High relative speed due to opposite course of target and sonar platforms in conjunction with the 12 s signal duration created a highly dynamic geometry. The effect this geometry has on the signal/data processing will be addressed analytically in section 5.

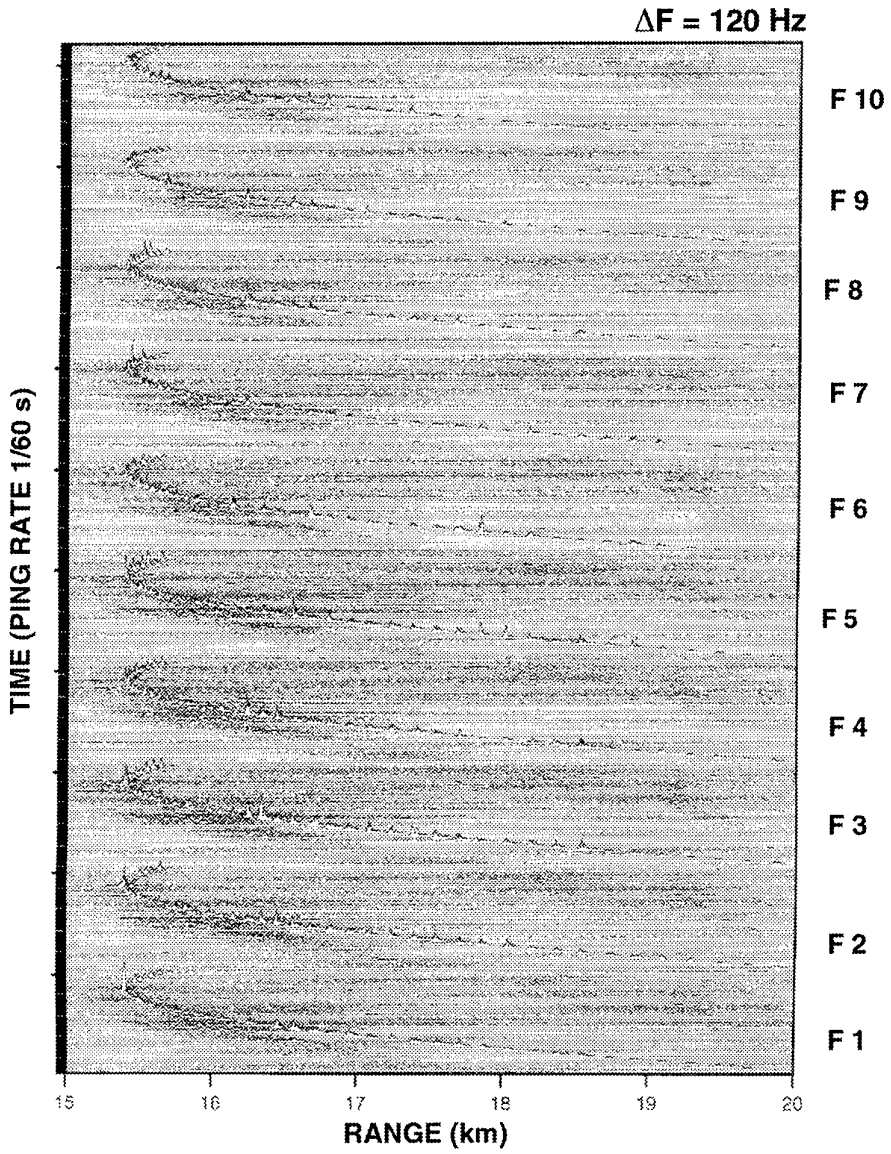

Figure 6: Frequency dependent sub-band matched filter processing. Unnormalized output from ten sub-bands arranged with increasing frequency order from bottom F1(2300-2420 Hz) to top F10 (3380-3500 Hz).

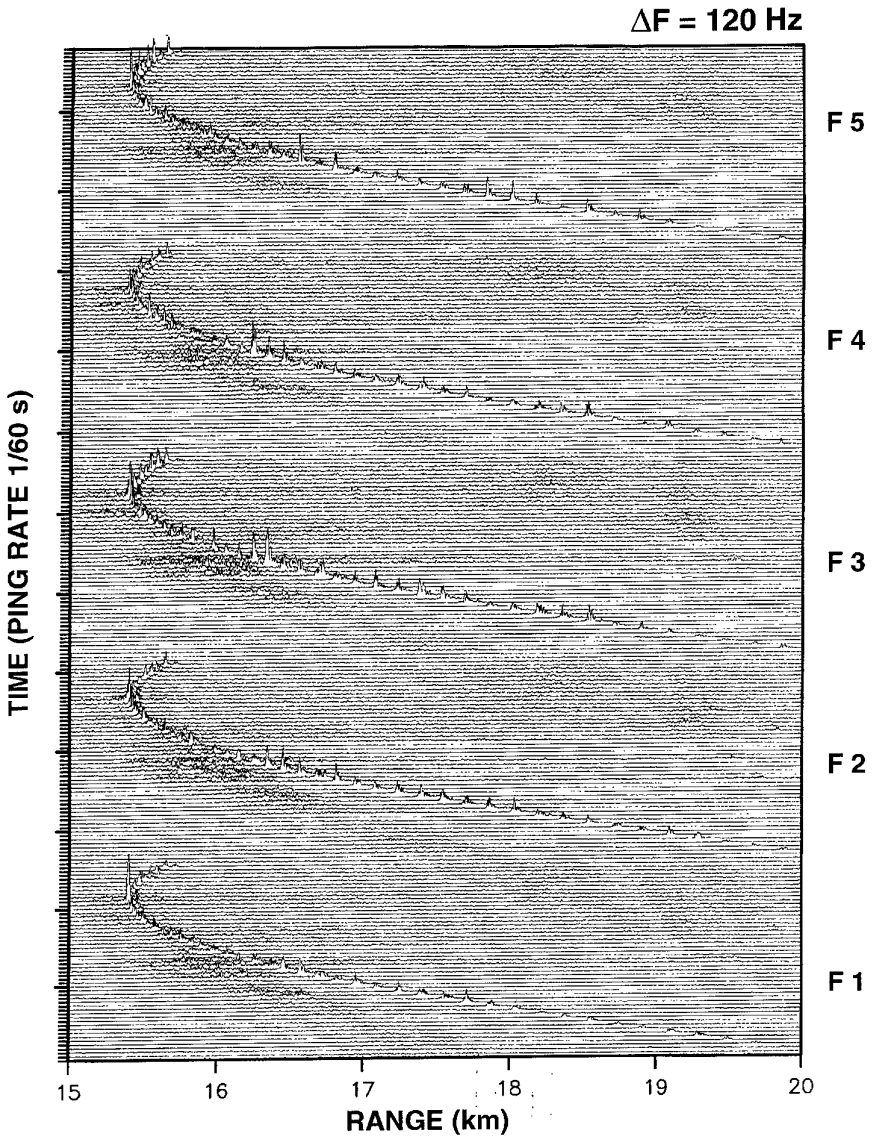

Figure 7: Frequency dependent sub-band matched filter processing. Unnormalized output from the first five sub-bands arranged with increasing frequency order from bottom F1(2300-2420 Hz) to top F5 (2780-2900 Hz).

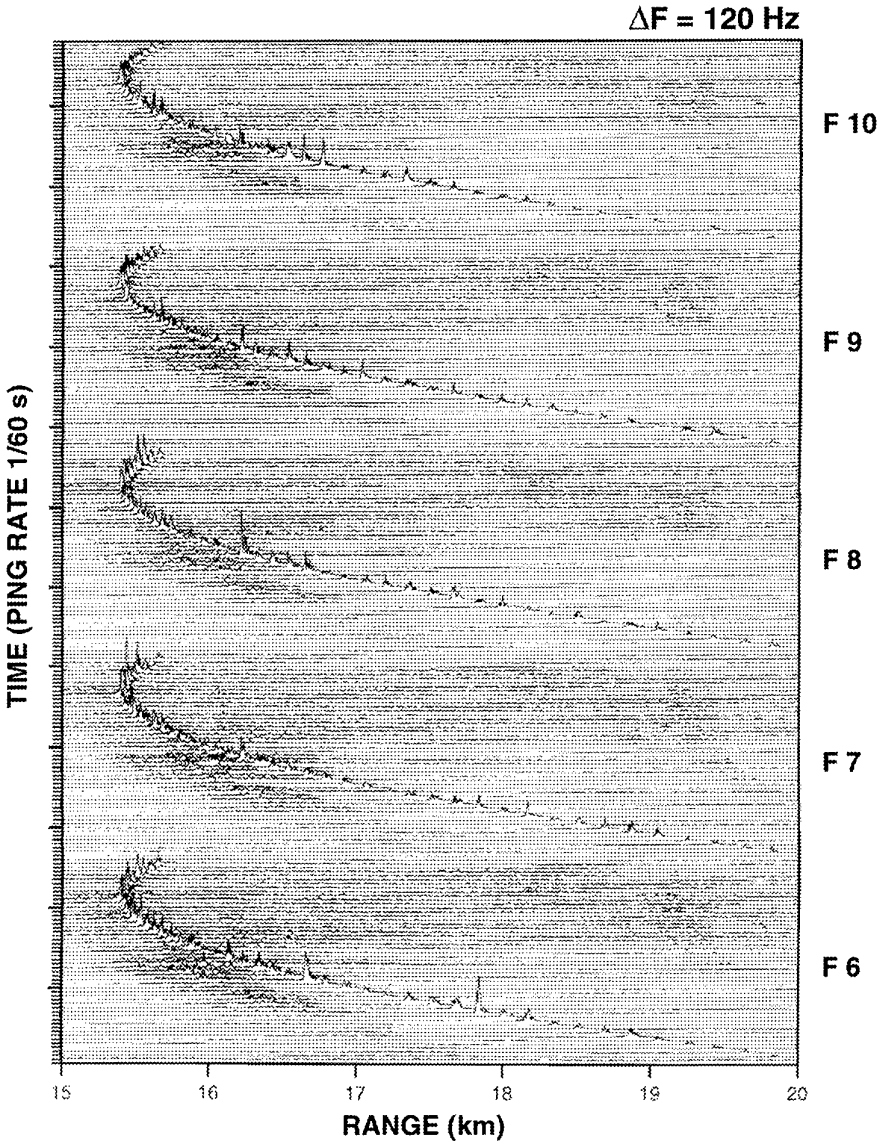

Figure 8: Frequency dependent sub-band matched filter processing. Unnormalized output from the first five sub-bands arranged with increasing frequency order from bottom F6 (2900-3020 Hz) to top F10 (3380-3500 Hz).

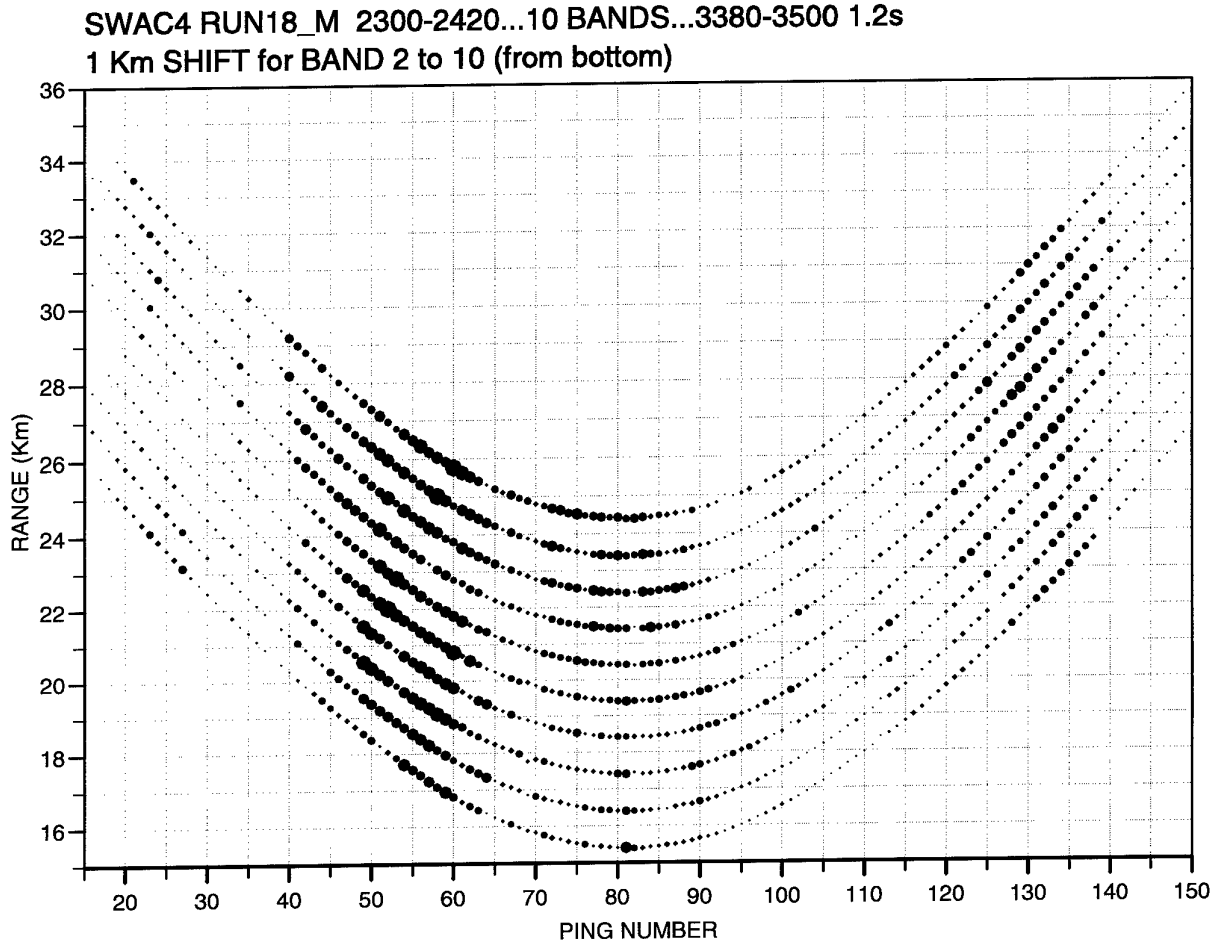

Figure 9: Target localization and signal-to-noise ratio as a function of frequency. The bottom curve represents actual range values. The other curves have a 1 km offset to avoid overlap. The size of the dot is proportional to the SNR and varies from 10 to 48 dB.

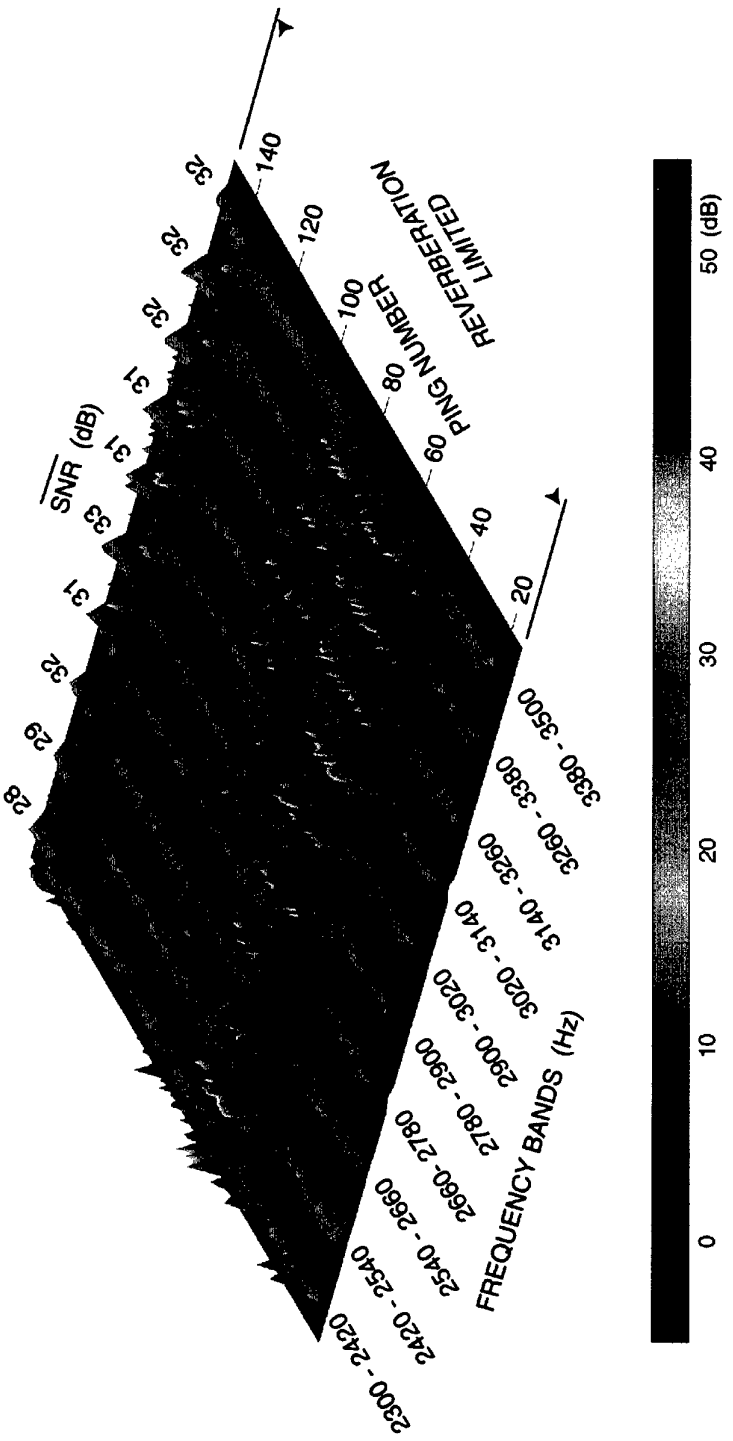

Figure 10: SNR as a function of frequency in a reverberation limited environment. For each sub-band, the average SNR for the entire run is indicated.

4

Sub-band SNR ratio comparison

The variation of SNR as a function of range and frequency is fundamental to the assessment of sub-band MF performance. The SNR is directly related to target detection and incorporates signal and noise variations. The value of SNR=10 dB is selected as the nominal detection threshold. Everything above this value is classified as a potential target. For the data presented here, everything above 10 dB is verified to be the target.

Figure 11 shows the SNR variation corresponding to the ten sub-bands as a function of ping number, which can be related to time and range, given that the ping repetition rate is one minute and the source speed is 5 knots. For each ping, the bar length represents the SNR value span in the ten sub-bands. The black bars indicate that all ten values are greater than the 10 dB detection threshold while the grey bars correspond to cases where the SNR in one or more sub-bands is below this threshold. Figure 11 demonstrates the fluctuations of the SNR over 130 pings. Similarly to the target ranging (Fig. 9), the maximum SNR values correspond to the closing part of the run (pings 40-60) before the CPA (ping 80). It can also be observed that there are three areas of local minima at ping numbers 25, 105 and 145. To explain these SNR variations and to see the individual contribution of each sub-band, two steps are taken: the signal and the noise calculations are separated and the SNR values for three characteristic sub-bands are plotted individually. The SNR values for the lowest (2300- 2420 Hz), the middle (2780-2900 Hz) and the highest (3380-3500) band are superimposed on the general plot (Fig. 12, 13, and 14). It may appear that the low frequencies have low SNR values, however this is not true for the first 40 pings. The middle frequencies indicate more local maxima than the high frequency sub-band. In conclusion, the SNR fluctuations do not appear to be frequency dependent.

The SNR pattern, signal and the noise calculations are plotted separately in Fig 15. The top "cluster" part of the plot corresponds to the signal values and the bottom "cluster" part shows the noise levels in dB. For each ping, only those signal and noise estimates which correspond to SNR greater that 10 dB are plotted. It can be observed that the signal values are symmetric around the CPA maximum. This also indicates that good propagation conditions result in two-way intensity levels proportional to the distance between source and receiver. On the contrary, the noise characteristics vary with respect to range. At the beginning of the run, the

noise values are high due to ship traffic and reverberation followed by a low noise area, at the end of the run a noise increase is observed.

This is a first approach at broadband data analysis therefore we concentrated only on the SNR variation to assess the detection performance. Future investigation will utilize Receiver Operating Characteristics (ROC) curves as standard measure of performance.

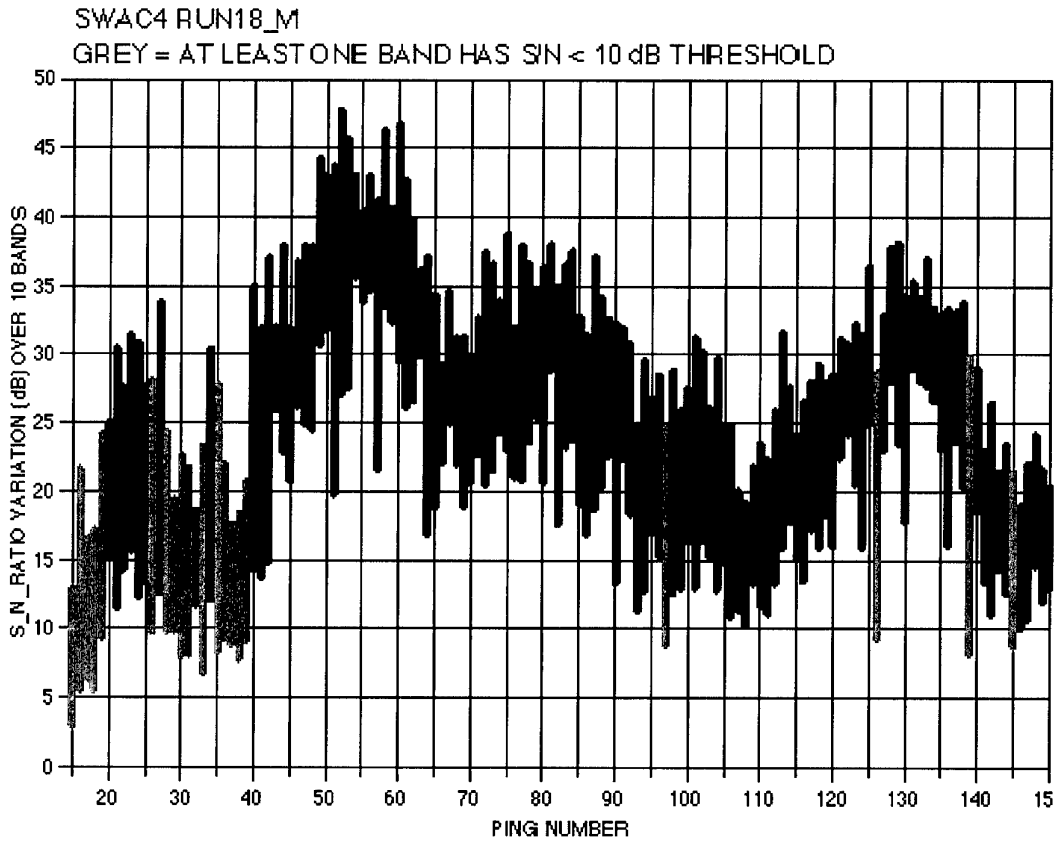

Figure 11: SNR versus ping number. Each vertical bar corresponds to the SNR variation of the ten sub-band estimates. Black bars indicate that all ten SNR values are above the detection threshold of 10 dB while grey bars indicate that one or more SNR values are below this threshold.

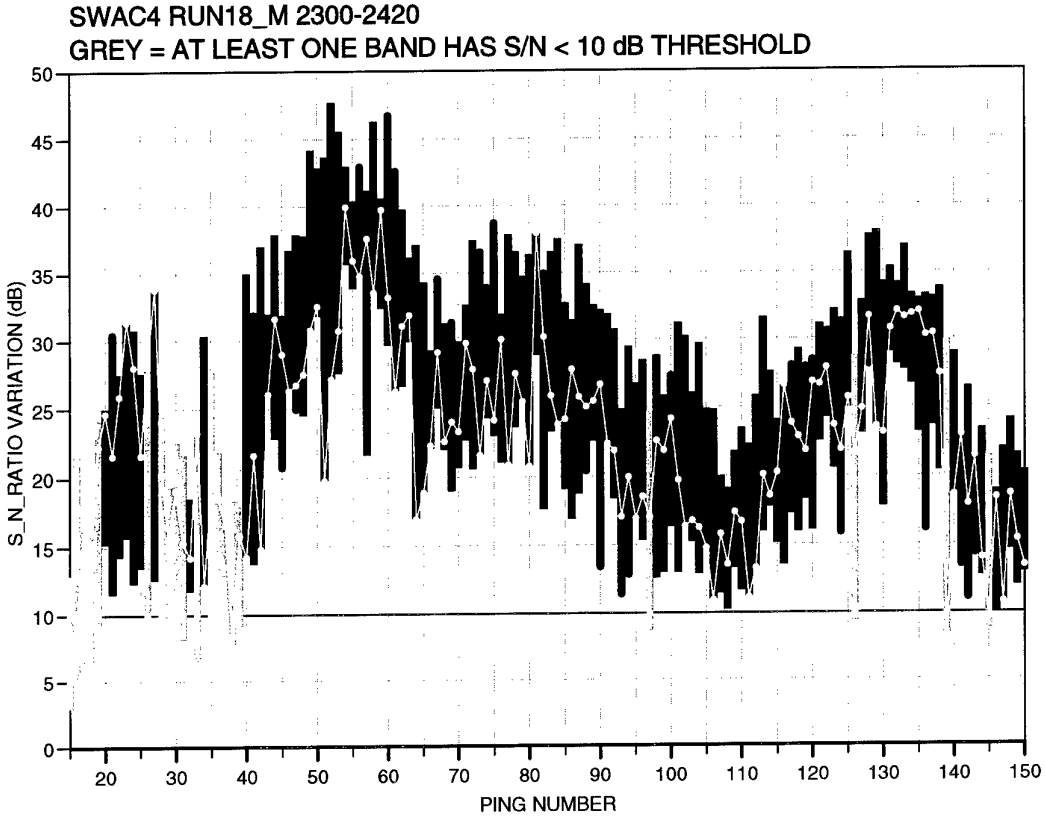

Figure 12: SNR versus ping number for the lowest frequency sub-band (2300-2420 Hz). The yellow line indicating the SNR values for the particular band is superimposed on the general plot of Fig. 11.

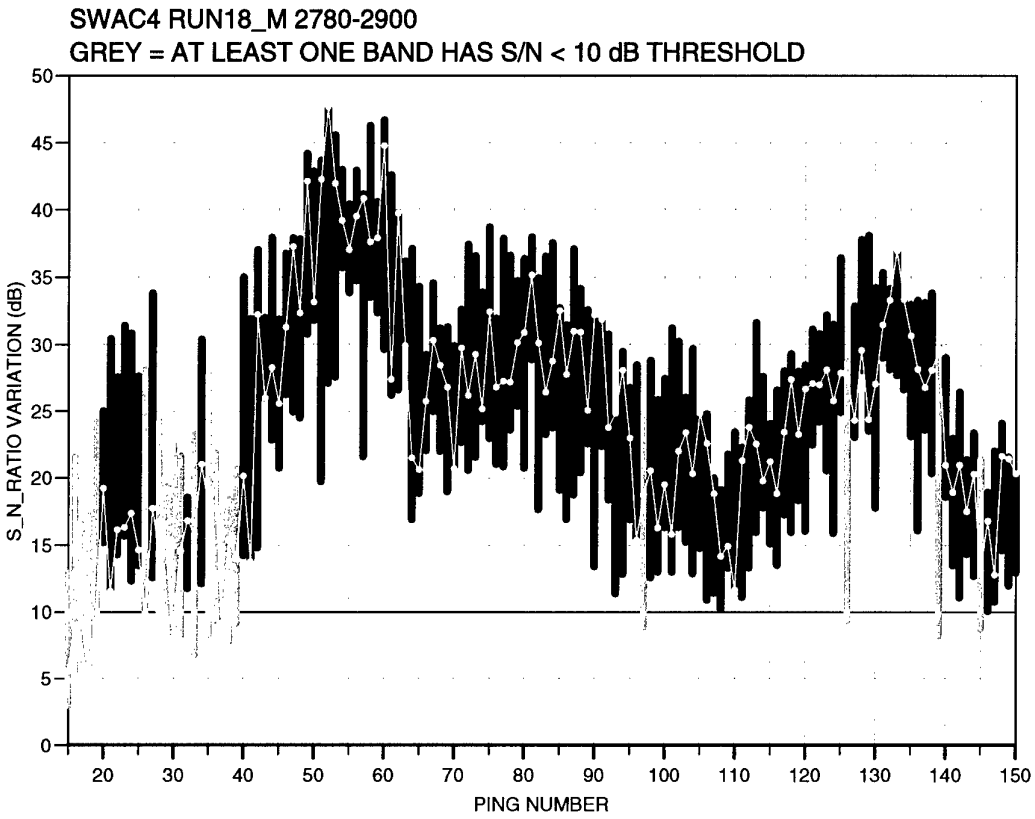

Figure 13: SNR versus ping number for the lowest frequency sub-band (2780-2900 Hz). The green line indicating the SNR values for the particular band is superimposed on the general plot of Fig. 11.

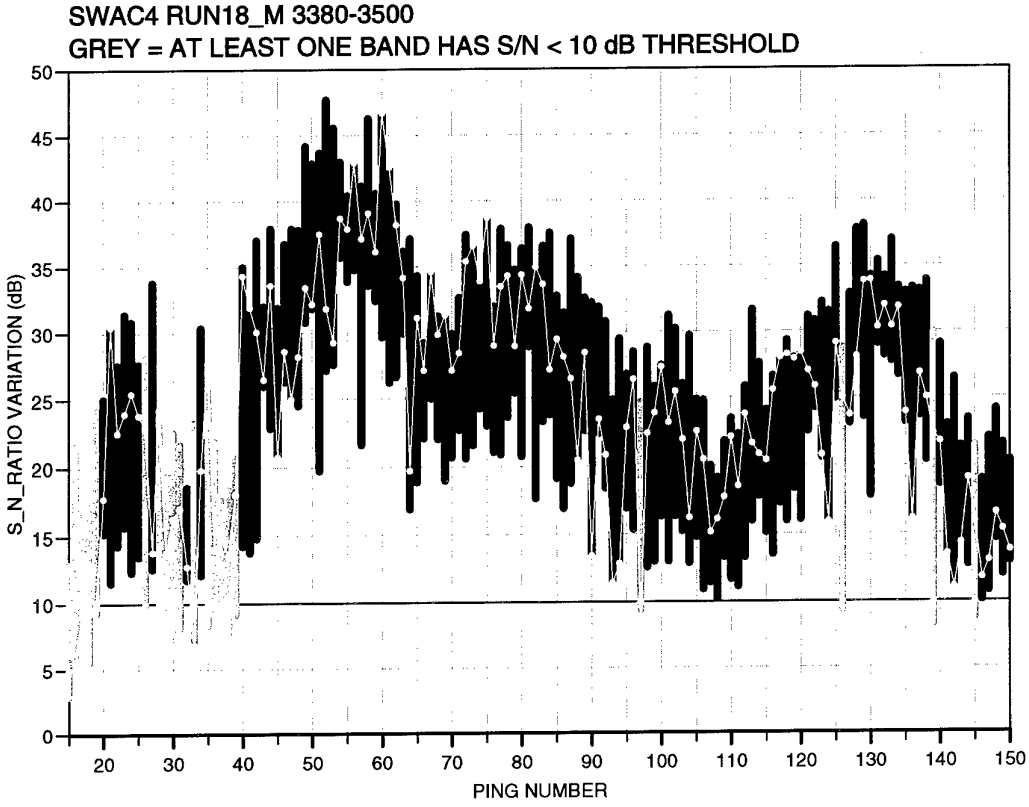

Figure 14: SNR versus ping number for the lowest frequency sub-band (3380-3500 Hz). The blue line indicating the SNR values for the particular band is superimposed on the general plot of Fig. 11.

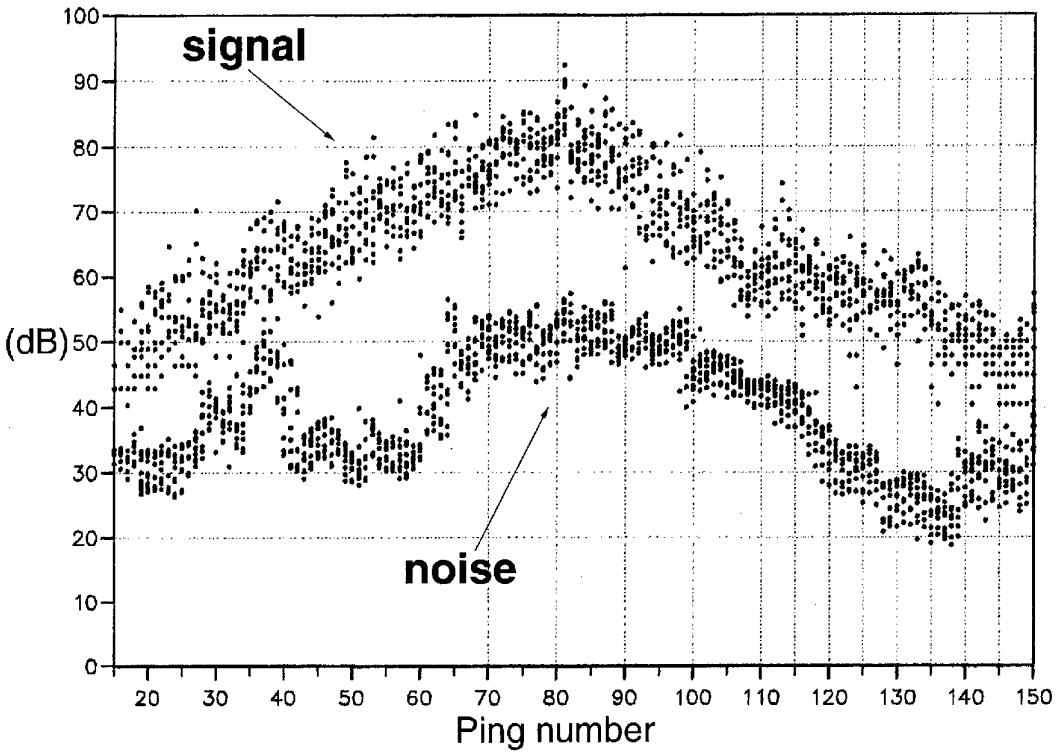

Figure 15: Separate estimates for signal and noise versus ping number. Their pattern implies that the SNR variations shown in Fig. 11, 12, 13, and 14 are attributable to noise fluctuations.

5

Doppler effect and sub-band detection differential time delay

This section deals with the Doppler effect on active detection performance caused by relative motion between source and target and exacerbated by long-duration transmissions. The problem of sub-band synchronization regarding MF incoherent processing, is also addressed.

In general, the resolution cell in active sonar cases can be expressed in the following way:

$$v_r T = \frac{c}{2B} \tag{1}$$

therefore the range rate is given by the formula

$$v_r = \frac{c}{2\ BT} \tag{2}$$

where v_r is the relative velocity or range rate between source and receiver in meters, c is the sound speed in m/s, B is the signal bandwidth in Hz, and T is the duration of the pulse in seconds.

In particular, it can be shown that the velocity tolerance of an LFM, which is defined as the relative velocity value corresponding to a $-3dB$ correlation loss is given by the following equation [1]

$$v_r = \frac{1350}{BT} \tag{3}$$

where v_r is the range rate in m/s.

In run 18 the total duration of the LFM pulse is 12 s and the total bandwidth is 1200 Hz. Eq. (3) indicates that the velocity tolerance is practically zero. In reality, the source and the target are moving towards or away from each other on a parallel course with an average relative velocity of 8.6 kn. Thus a severe Doppler problem exists.

The frequency shift caused by the Doppler effect can be calculated using the following formula [2]

$$\Delta f = \pm \frac{2v_r}{c} f \tag{4}$$

where f the operating frequency in Hz. The $\pm$ sign indicates up-Doppler for approaching and down-Doppler for receding targets. For an average relative speed of 8.6 Kn and for the minimum frequency 2.3 kHz, the frequency shift is 19.78 Hz.

According to Eq. (3), sub-band MF detection, is not significantly affected by the Doppler effect because each band width is 120 Hz with corresponding sub-pulse duration 1.2 s. However, two synchronization problems arise when incoherently processing the received signal. The first one is the 1.2 s time delay between adjacent sub-band outputs. This time lag becomes more evident considering the 10.8 s delay between first and last sub-band. When all ten sub-band detection outputs are incoherently processed this time delay must be accounted for. The second problem is related to the geometry of the run which creates a continuous range change between source and receiver. At the closing part of the run, the distance between source and receiver is reduced during the 12 s transmission and *vice versa*, it is increased during the opening part of the run. Contrary to the well-defined transmission delay between adjacent sub-bands, the differential time delay is a more subtle phenomenon.

Figure 16 demonstrates this problem caused by source and target repositioning during transmission. The 1.2 s difference between adjacent sub-bands has already been taken into account, therefore what is shown here is the two-way travel time of the transmitted sub-pulse. Eleven plots are included. From bottom to top, the first ten plots show the MF output for ping 45 *versus* detection time, arranged in increasing frequency (sub-band) order. The top plot shows the normalized average of the ten sub-bands plotted below it. The y-axis represents the MF output normalized according to the SNR for each sub-band. Their normalized average is smoother than the individual output series and it reaches its maximum at the median of the individual sub-band maxima. Figure 16 corresponds to the closing part of the run during which distance between target and receiver is reduced. Detection outputs based on high

frequency sub-bands indicate reduced detection times. This is explained by the fact that the high frequencies in the 12 s pulse are transmitted last (up-sweep pulse), therefore, at that point, the distance between source and target is reduced relative to the beginning of the transmission. On the contrary, during the opening part of the run the distance between source and receiver increases during transmission. At the CPA, the distance between target and receiver does not change significantly thus the detection time remains the same for all ten sub-bands. The next chapter includes a method to exploit this differential time delay in order to estimate the range rate between source and target based on a single ping observation.

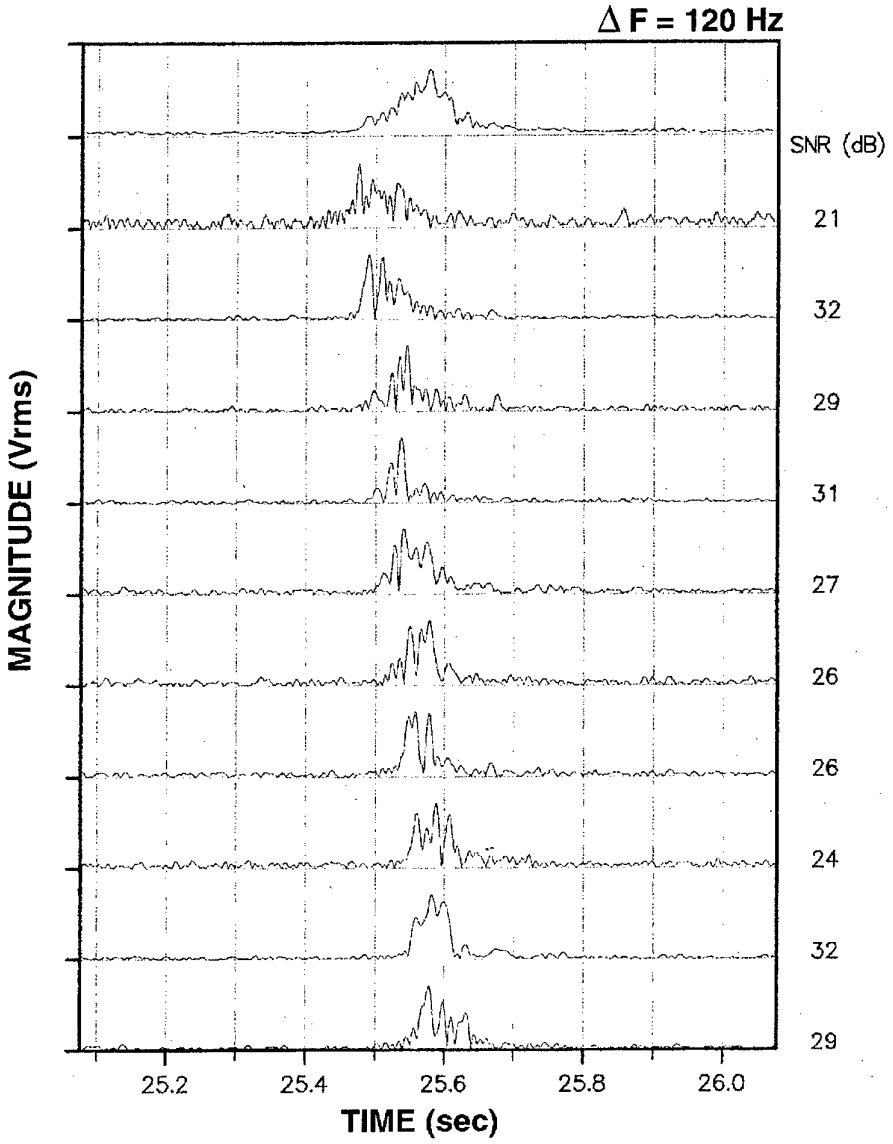

Figure 16: Normalized MF output for ping 45 (closing part of the run) with SNR estimation for each sub-band independently. The sub-band differential time delay is shown. The top plot shows the normalized average of the individual sub-band MF outputs.

6

Range rate estimation based on intra-ping sub-band differential time delay

Sub-band MF processing and in particular the differential detection time delay discussed in the previous section provides sufficient information to estimate the relative velocity between source and receiver. This alternative intra-ping scheme presented here is suitable when the standard inter-ping method is not applicable due to the absence of ping history.

Let R_m and R_n denote the detection distances corresponding to sub-bands m and n. The time interval between sub-bands m and n is T_{mn}. Then the intra-ping range rate is given by the following formula:

$$u = \frac{R_m - R_n}{T_{mn}} \tag{5}$$

The sub-band detection times corresponding to R_m and R_n are denoted dt_m and dt_n respectively. After substitution of $R_m = dt_m c/2$ and $R_n = dt_n c/2$ into Eq. 5, the intra-ping range rate formula becomes

$$u = \frac{c}{2}\frac{DT_{mn}}{T_{mn}} \tag{6}$$

where $DT_{mn} = dt_m - dt_n$ is the differential detection time delay between sub-bands m and n, and c (m/s) is the sound velocity in the water column.

For example, the range rate estimation based on the two extreme sub-bands proceeds as follows: m=1 (first sub-band), n=10 (last sub-band), $T_{mn} = 10.8s$, $c = 1511m/s$, and for ping 45 $dt_m = 25.577s$, $dt_n = 25.475s$. Substitution of these values into Eq.(6) gives the following intra-ping range rate value:

$$u = \frac{0.102}{10.8} \frac{1511}{2} = 7.135\ m/s \tag{7}$$

where $DT_{mn} = dt_m - dt_n = 25.577 - 25.475 = 0.102\ s$ is the sub-band differential delay between the first and the last band.

It is noted that 7.135 m/s is approximately 14 *knots*; too large for the relative velocity of two platforms having average speed 5.2 *knots* each. Figure 17 shows inter-ping (blue line) range rate estimation, the average intra-ping range rate estimation (red line) for the entire run and individual estimates intra-ping estimations (black lines) based on different sub-band pairs. Obviously there is a significant difference between the two estimates as the intra-ping values are almost double the inter-ping ones. This relationship is explained in the following subsection.

6.1 *Inter-ping* versus *intra-ping range rate estimation*

The difference between the two estimates is due to the fact that the intra-ping range rate estimate is attributed not only to distance change, as mentioned above, but also to an additional Doppler shift which occurs during the transmission of a single ping. This frequency shift creates a different compression and expansion detection time for each sub-band. For LFM signals the time change corresponding to the frequency offset due to relative velocity can be expressed in the following way [13]:

$$\Delta\tau_1 = \frac{2u_r}{c} \frac{T_s}{B_s} f_1 \tag{8}$$

where u_r is the actual (inter-ping) range rate, c is the sound speed, f_1 is the central frequency, T_s is the duration of the sub-pulse, B_s is the bandwidth of the sub-band.

Then, the delay between two sub-bands can be written as:

$$\Delta\tau = \Delta\tau_1 - \Delta\tau_2 = \frac{2u_r}{c} \frac{T_s}{B_s} (f_1 - f_2) \tag{9}$$

where f_2 is the central frequency of the second band. Note that all sub-bands have the same bandwidth B_s and duration T_s.

The additional range rate factor which corresponds to this time difference between sub-bands is given by the formula:

$$\Delta v_r = \frac{c\,\Delta\tau}{2\,T_T} \tag{10}$$

where T_T is the transmission time difference between the two sub-bands.

Using Eq. (9), Δv_r becomes

$$\Delta v_r = v_r \frac{T_s}{B_s} \frac{(f_1 - f_2)}{T_T} \tag{11}$$

For an LFM signal, frequency changes proportionally to time, so

$$\frac{T_s}{T_T} \approx \frac{B_s}{(f_1 - f_2)} \tag{12}$$

where the $\approx$ sign indicates that $(f_1 - f_2)$ is approximately the bandwidth which corresponds to T_T.

Equation (12) in conjunction with Eq. (11) leads to

$$\Delta v_r = v_r \tag{13}$$

which means that the additional range rate factor due to Doppler equals the actual range rate.

In other words, the intra-ping estimation of the range rate given by Eq. (6) is twice the actual range rate. So, it is shown that for an LFM signal the relationship between intra-ping v and inter-ping (actual) v_r range rate estimation is

$$v = 2v_r \tag{14}$$

The application of this formula to the real data is shown in Fig. 18 where the intra-ping range rate calculation offers an accurate estimation of the actual relative velocity between source and receiver.

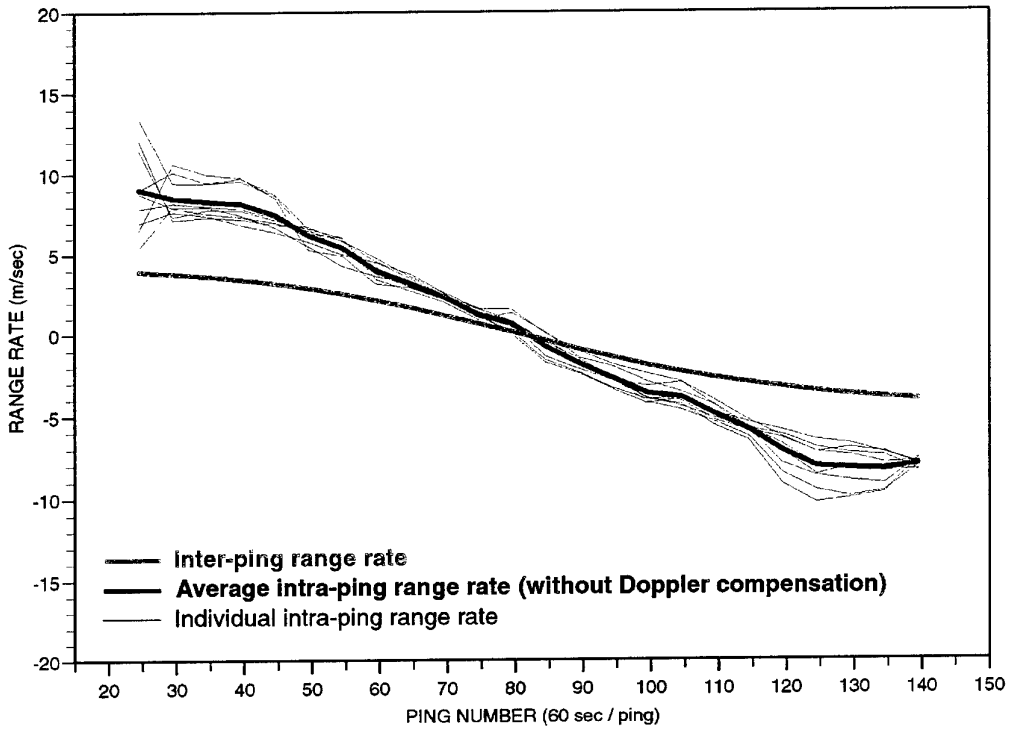

Figure 17: Before the correction for the intra-ping Doppler effect: the actual, inter-ping range rate estimate (blue line) compared to the average range rate estimate (red line) of nine independent calculations (black lines) based on different sub-band pairs.

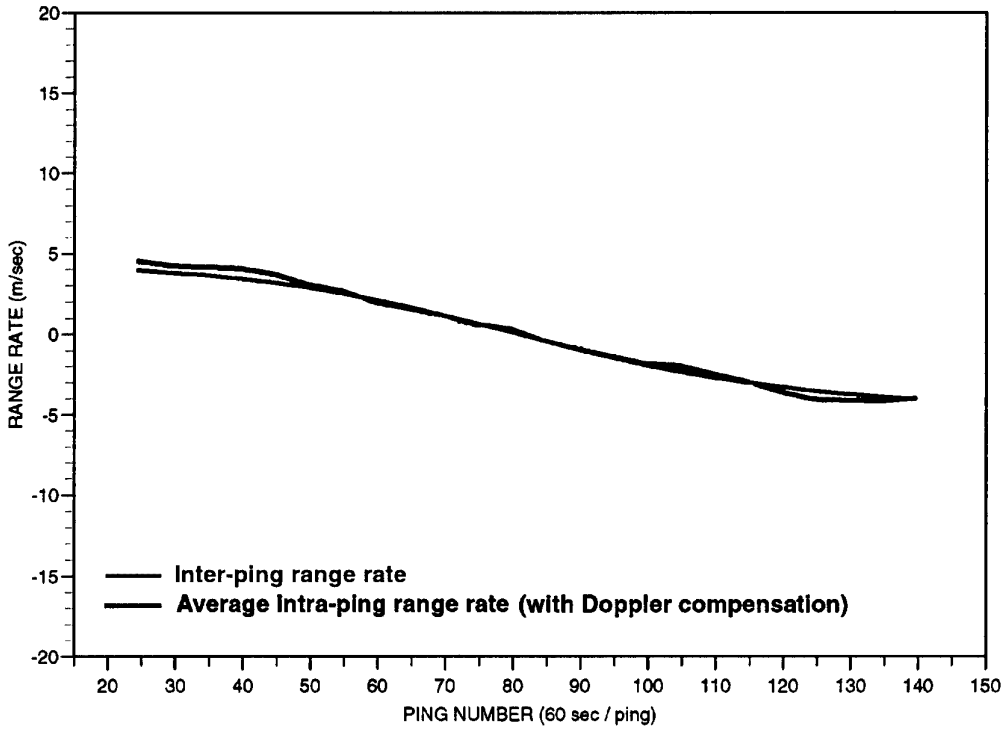

Figure 18: After the correction for the intra-ping Doppler effect: the actual, inter-ping range rate estimate (blue line) compared to the average range rate estimate (red line).

7
Conclusions

The conclusions drawn from this work are both case-specific and general. For example, results related to the type of run should not be generalized, and *vice versa*, the analysis of long pulse duration effects can be assessed in a more general framework. This distinction is necessary because the data set analyzed here was acquired during a sea trial which did not have broadband analysis as its main objective. This created certain inconveniences which may be avoided in future experiments specifically planned for wide band signals utilization.

To examine the frequency dependence of detection performance for broadband signals, a sub-band processing scheme was deviced. The transmitted spectrum was divided into ten sub-bands of equal length which are processed independently. The comparison among sub-band MF outputs indicates a small degree of frequency dependence for the particular data set. However, ping-to-ping variations of local sub-band maxima suggest potential performance gain for incoherent processing schemes. In processing sub-bands incoherently, the detection time shift between adjacent bands is estimated. This offset is generated as the distance between source and receiver changes during transmission. The compensation for this time shift may improve the performance of MF methods by means of synchronizing the individual inputs in an incoherent processing algorithm. This scheme can be realized with precision when the target speed is known or when it can be accurately calculated. In the opposite case, which is what usually happens in operational scenarios, an *a priori* set of Doppler coefficients must be used to formulate a "synchronization" algorithm suitable for target Doppler estimation. This type of methods must take under consideration the fact that the sub-band MF outpus are completely uncorrelated as it appears from the normalized target echoes. On the contrary, their normalized average, which peaks at the median value of the sub-band maxima, has a less fluctuating envelope than the individual sub-band time series.

The detection time delay due to the Doppler effect is exploited for the estimation of the relative velocity between source and receiver based on different sub-bands of the same ping (intra-ping range rate estimate). The relationship between intra-ping and inter-ping estimation is also derived.

Although the utilization of wide band signals may offer significant detection advantages, broadband processing is particularly susceptible to the Doppler effect. The

frequency shift caused by relative velocity between source and receiver is frequency dependent itself and is exacerbated by long duration signals. This renders wide band Doppler compensation a complicated task. For research purposes, one way to minimize the Doppler effect in order to focus on the increased bandwidth processing aspect of the problem is to design the experiment so that source and receiver move in a parallel course with the same direction.

With respect to fleet oriented applications, it should be emphasized that long duration transmission creates significant operational disadvantages. The present results may be used to demonstrate the following point: during the 12 s transmission the hydrophones are overloaded due to a combination of the direct arrival and reverberation; this creates a "blind range" of approximately 9 km. The longer the pulse, the longer the "blind range". Target detection methods are most likely to fail at this range. It is recommended that when operational scenarios demand the utilization of long pulses (e.g. for energy increase), to alternate these signals with shorter pulses (which provide better near field detection capabilities) in order to control possible target presence at close range.

Future plans in broadband processing include the generation of ROC curves as a standard measure of performance and analysis of the frequency dependence of both detection and false alarm probability.

The SACLANT Undersea Research Centre provides the Supreme Allied Commander Atlantic (SACLANT) with scientific and technical assistance under the terms of its NATO charter, which entered into force on 1 February 1963. Without prejudice to this main task - and under the policy direction of SACLANT - the Centre also renders scientific and technical assistance to the individual NATO nations.

SACLANT Undersea Research Centre
Viale San Bartolomeo 400
19138 San Bartolomeo (SP), Italy

tel: +39 0187 527 (1) or extension
fax: +39 0187 527 700

e-mail: library@saclantc.nato.int

NORTH ATLANTIC TREATY ORGANIZATION